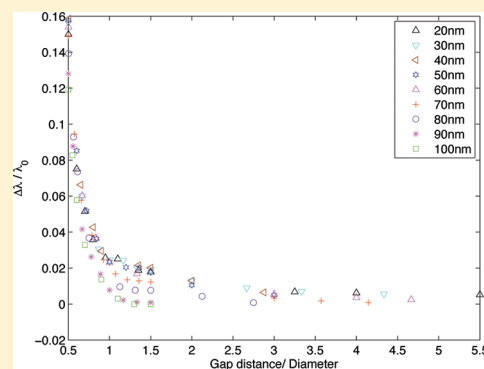


Size Dependence of the Plasmon Ruler Equation for Two-Dimensional Metal Nanosphere Arrays

Xue Ben and Harold S. Park*

Department of Mechanical Engineering, Boston University, Boston, Massachusetts 02215, United States

ABSTRACT: We have utilized the discrete dipole approximation to study the localized surface plasmon resonance in infinite, periodic two-dimensional arrays of gold nanospheres with the nanospheres arranged according to the {100} face of an *fcc* crystal. Specifically, we have performed a systematic study of the sensitivity of both the plasmon resonance wavelength shift and extinction properties considering nanosphere diameters ranging from 20 to 100 nm, and for nanosphere gap distances ranging from 0.5 to 6 times the nanosphere diameter. In doing so, we find that the same universal decay length of the plasmon resonance wavelength shift of about 0.2 units of the nanosphere size that was previously found by Jain et al.¹ for nanoparticle dimers is also operant for two-dimensional arrays. However, we also find that the universality of the plasmon ruler is only valid for arrays with nanospheres smaller than a critical nanosphere diameter of about 70 nm, whereas for larger nanosphere diameters, a decrease in the extinction efficiency as the gap distance decreases and a reduction in the decay constant are observed. Both of these size-dependent optical responses are qualitatively interpreted using a semianalytical coupled dipole approximation that accounts for structural retardation due to the geometric arrangement of the nanospheres, as well as single sphere retardation due to both dynamic depolarization and radiative damping effects. Using the semianalytical theory, we find that the size dependence is primarily due to the effects of dynamic depolarization and structural retardation, which reduces the coupling strength, changes the extinction efficiency trend, and also reduces the decay constant of the plasmon ruler equation for larger diameter nanospheres; similar results were found for infinite, 2D arrays of nanospheres in hexagonal and simple cubic arrangements. Finally, the semianalytical theory is utilized to predict a size dependence of the plasmon ruler for dimers starting at the same critical diameter of 70 nm. However, we find that the size effect is weaker for dimers than for the array case due to the significant reduction in structural retardation for dimers as compared to the array case.



INTRODUCTION

The optical properties of *fcc* metal (gold and silver) nanostructures have recently been the focus of intense scientific study. The driving force for the interest is because, upon interaction with incident electromagnetic waves, such as light, these metal nanostructures exhibit localized surface plasmon resonance (LSPR).^{2–4} The LSPR results in both an enhancement of the near-field electromagnetic fields,^{5–7} with potential Raman enhancements of up to 10¹², and the far-field optical efficiencies,^{8–10} with applications in optical sensing and imaging,^{11–15} miniaturized photonic devices,^{2,16,17} and photothermal cancer therapies,^{18–20} among many others.

Many of these optical applications involve not an individual nanoparticle, but collections, or arrays of the nanoparticles that are arranged in a manner such that the optical properties can be enhanced and exploited.^{21–23} Two examples of this are the enhancement in electromagnetic fields that can occur at nanometer separations between individual nanoparticles that is useful for single molecule sensing and detection,^{5,24,25} and the utilization of multidimensional arrays and arrangements of nanostructures for enhanced plasmon coupling and biosensing applications.^{15,26,27}

Because of this, there have been many studies, both experimental^{28–39} and theoretical,^{23,40–49} that have investigated the optical properties of either dimers or one and two-dimensional (2D) arrays of *fcc* metal nanoparticles, though it should be noted that the vast majority of such studies, both experimental and theoretical, has focused on the far simpler dimer geometry.

One key issue that was recently resolved for the case of interacting nanoparticle dimers was the development of an analytic expression for the dependence of the far-field optical properties and, specifically, the LSPR wavelength shift as a function of nanoparticle size and the gap between the nanoparticles. Such information is necessary to systematically optimize the arrangements of nanoparticles with predictable and repeatable optical properties for optical sensing applications. Specifically, Sonnichsen et al.⁵⁰ and Reinhard et al.⁵¹ established a “plasmon ruler” to measure distances in biological systems based on the change in optical properties that result from the

Received: June 13, 2011

Revised: July 11, 2011

Published: July 12, 2011

interaction of two nanoparticles. The plasmon ruler was given an analytic form for the case of gold nanodisc dimers by Jain et al.,¹ who also found a nearly universal scaling of the decay length of the interactions between nanoparticle dimers that was apparently independent of nanoparticle size, shape, metal type, and dielectric constant. This plasmon ruler equation was then used to explain the experimental results of Reinhard et al.⁵¹

The objective of the present work is to move beyond the case of nanoparticle dimers and develop a plasmon ruler equation for infinite 2D periodic arrays of gold nanospheres such that the spectral shift that occurs for arrays of metal nanospheres can be predicted not only as a function of the interparticle separation but also as a function of the nanoparticle size. We expect that this theoretical information should be valuable considering the recent experimental advances that have demonstrated the capability of mechanically tuning the distances or gap between metal nanostructures,^{52–54} in conjunction with well-established experimental techniques, such as nanosphere lithography²¹ or Langmuir–Blodgett assembly,²² that suggest that experimental studies of periodic arrangements of nanoparticles with arbitrary nanoparticle sizes and tunable gap distances between the particles are certainly within reach.

We accomplish this through numerical calculations based on the discrete dipole approximation (DDA)^{55,56} and semianalytical expressions based upon an extension of the coupled dipole approximation (CDA)⁴⁴ that accounts for size-dependent single sphere retardation via both dynamic depolarization (DD) and radiative damping (RD) effects.^{30,38,57} We utilize both approaches to study the changes in LSPR wavelength that occur for an infinite 2D array of gold nanospheres with diameters up to 100 nm and gap distances ranging from 0.5 to 6 times the nanosphere diameter. Together, the DDA and semianalytic CDA expressions enable us to conclude that the universal decay constant that was previously found for nanodisk dimers by Jain et al.¹ holds only for nanosphere diameters smaller than about 70 nm. For larger diameter nanosphere arrays, we find using the CDA that DD and structural retardation are the major factors determining the size-dependent behavior of the coupling strength and extinction efficiency, and the reduced decay constant in the plasmon ruler equation for larger diameter nanospheres. Similarly, we also find a size dependence of the plasmon ruler starting at the same critical diameter of 70 nm for the dimer case. However, the size dependence is far weaker as compared to the array case due to the significant reduction in structural retardation for the dimers.

NUMERICAL METHODOLOGY

To calculate the extinction spectra for an infinite, periodic 2D array of gold nanospheres, we utilize the discrete dipole approximation (DDA), which was originally developed by Purcell and Pennypacker.⁵⁵ The fundamental idea behind the DDA is to discretize a volume of arbitrary geometry using small (finite) elements, in which each element represents an individual dipole with polarizability α_i that interacts, due to an incident electric field, with all other dipoles in the body. The polarization can be written as¹⁰

$$\mathbf{P}_i = \alpha_i \mathbf{E}_{\text{loc},i}(\mathbf{r}_i) \quad (1)$$

where the local electric field $\mathbf{E}_{\text{loc},i}$ is the sum of an incident field $\mathbf{E}_{\text{inc},i}$ and the contribution from the j other dipoles in the system

$\mathbf{E}_{\text{other},j}$ and can be written as

$$\mathbf{E}_{\text{loc},i} = \mathbf{E}_{\text{inc},i} + \mathbf{E}_{\text{other},j} = \mathbf{E}_0 \exp(i\mathbf{k} \cdot \mathbf{r}_i) - \sum_{j \neq i} \mathbf{A}_{ij} \cdot \mathbf{P}_j \quad (2)$$

where \mathbf{k} is the wave vector of the incident plane wave, \mathbf{E}_0 is the amplitude of the plane wave, and the matrix \mathbf{A}_{ij} represents the interactions of all dipoles i and j as

$$\mathbf{A}_{ij} \cdot \mathbf{P}_j = \frac{\exp(ikr_{ij})}{r_{ij}^3} \left(k^2 r_{ij} \times (r_{ij} \times \mathbf{P}_j) + \frac{1 - ikr_{ij}}{r_{ij}^2} \times (r_{ij}^2 \mathbf{P}_j - 3r_{ij}(r_{ij} \cdot \mathbf{P}_j)) \right) \quad (3)$$

The goal of the DDA is to solve for the polarization vector \mathbf{P} in eq 2. Once this is known, the extinction cross section can be calculated as⁵⁸

$$C_{\text{ext}} = \frac{4\pi k}{|\mathbf{E}_0|^2} \sum_{j=1}^N \text{Im}(\mathbf{E}_{\text{inc},j}^* \cdot \mathbf{P}_j) \quad (4)$$

In the present work, we calculate the extinction spectra for infinite, periodic 2D arrays of gold nanospheres using the code DDSCAT by Draine and Flatau⁵⁶ and the dielectric constants of Johnson and Christy,⁵⁹ where, in particular, we utilize DDSCAT 7.0 due to its capability to calculate both near- and far-field optical properties for periodic arrangements of metal nanoparticles. We note that earlier versions of DDSCAT have recently been utilized by many researchers^{1,6,8,10,60–63} to study the extinction spectra of both individual metallic nanostructures and metal nanostructure dimers. We also note that nonlocal effects, which may be important for interactions of multiple nanostructures at very short particle separations,^{64,65} were not considered in the present work.

NUMERICAL RESULTS

The model infinite, periodic 2D array of gold nanospheres that we considered in the present work is one in which the positions of the nanospheres correspond to the atomic positions on the $\{100\}$ face of an *fcc* crystal. Nanosphere diameters ranging from $D = 20$ – 100 nm were utilized to study the LSPR wavelength shifts as a function of size, where air was the dielectric medium of choice for all calculations. Gap distances, which are defined as the edge-to-edge distance between two nanospheres along the $[100]$ direction on the $\{100\}$ *fcc* face, ranged between 0.5 and 6 times the nanosphere diameter. We note that, for our particular 2D periodic arrangement, the smallest possible gap distance is $(\sqrt{2} - 1)D$; the smallest center-to-center distance between the nanospheres is $\sqrt{2}D$. Touching spheres were not considered in our work due to the inapplicability of the DDA to such situations. The wave vector used in our calculations is perpendicular to the plane containing the infinite, periodic 2D array of nanospheres, whereas the polarization vector is parallel to the plane of the array and in the $[100]$ direction. This optical illumination is also utilized for the semianalytical CDA results presented later.

For these different nanosphere diameters and gap distances, the values of interest are the corresponding change in the far-field extinction properties and LSPR wavelength. We found that, for the 2D periodic array, different numbers of dipoles were required to obtain convergence of the LSPR wavelength, with more dipoles required to obtain convergence as the gap distance between nanospheres decreased. To ensure accuracy of the DDA

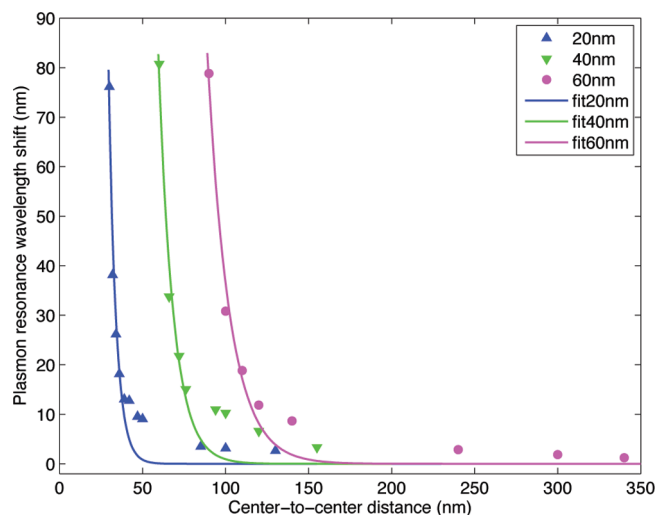


Figure 1. DDA calculations of LSPR wavelength shift versus gap distance for 2D infinite, periodic arrays with nanosphere diameters of 20, 40, and 60 nm. Solid curves are the least-squares fits to the function $y = a \exp -[(x - 1.414D)/(l)]$, where D is the nanosphere diameter. The corresponding decay lengths l are 4.5, 9.0, and 13.4 nm.

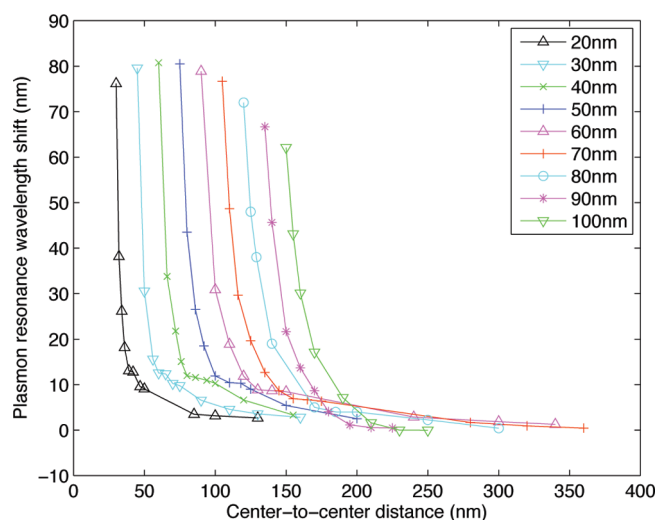


Figure 2. DDA calculations of LSPR wavelength shift versus gap distance for nanosphere diameters between 20 and 100 nm.

results, we performed a convergence study to ensure that, for each nanosphere diameter and gap distance, sufficient numbers of dipoles were used to obtain an accurate LSPR wavelength.

We show in Figure 1 the LSPR wavelength shift versus gap distance for 2D periodic arrays with nanosphere diameters of 20, 40, and 60 nm. We note that all LSPR wavelength shifts reported in this work for the arrays are red shifts with respect to the LSPR wavelength of the corresponding single nanoparticle. By fitting each of the curves separately, we find that the decay lengths increase with increasing nanosphere diameter, from about 4.5 nm when $D = 20$ nm, to about 13.4 nm when $D = 60$ nm. It is interesting to note that the 13.4 nm decay length we find for the infinite 2D periodic array with 60 nm diameter nanospheres is similar to the decay length of 13.7 nm found for the 54 nm diameter nanodisc dimers by Jain et al.¹ Furthermore, Figure 1 also shows that, for the same gap distance of $0.5D$, which

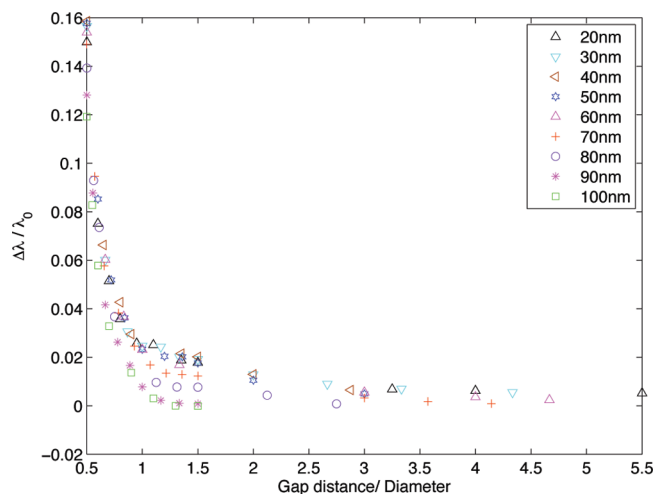


Figure 3. DDA calculations of scaled LSPR wavelength shift versus scaled gap distance for nanosphere diameters from 20 to 100 nm. It is clear that the data for arrays composed of 80, 90, and 100 nm nanospheres deviate from the universal exponential decay curve formed by the 20–70 nm nanospheres.

corresponds to the center-to-center distance $1.5D$, the magnitude of the LSPR wavelength shift increases from 20 to 40 nm and then decreases from 40 to 60 nm.

To examine the universality of our results, we systematically study the LSPR wavelength shift for nanosphere diameters from 20 to 100 nm; these results are summarized in Figure 2. One interesting finding is that, for the smallest gap distance of $0.5D$ (center-to-center distance of $1.5D$), there is, first, an increase in the maximum LSPR wavelength shift in going from about 20 to 50 nm, followed by a decrease for the 60–100 nm diameters. The behavior of the arrays with relatively small nanosphere diameters (<60 nm) thus appear to be reasonably well described by the dipolar electrostatic polarizability, which contains no size effects, where, due to the increase in volume, the absolute coupling strength increases as a result of the increased number of electrons that participate in the plasmon oscillation.

However, for the arrays with large nanosphere diameters between 60 and 100 nm, the size-independent dipolar polarizability loses accuracy. Because the nanosphere diameter becomes comparable to the incident wavelength of light, single sphere retardation effects in the form of DD and RD, which are size-dependent, compete with the volume increase and begin to confine the plasmon resonance more to the surface electrons, which reduces the overall oscillation strength per unit volume, and thus results in a smaller absolute plasmon coupling strength in this nanosphere size range.³⁹ This is shown most clearly in Figure 3, which demonstrates that, although the nanosphere diameters from 20 to 70 nm show a similar universal scaling for the normalized LSPR wavelength shift with gap distance, arrays with nanosphere sizes larger than 70 nm clearly deviate from the universal scaling exhibited by the smaller diameter arrays. This results from both single sphere retardation effects as well as structural retardation due to the geometric arrangement of the nanospheres. A further discussion delineating the relative importance of DD, RD, and the structural retardation within the context of the semianalytical CDA will be given later.

Figure 4 shows the scaled LSPR wavelength shift for all nanosphere diameters ranging from 20 to 70 nm on a single

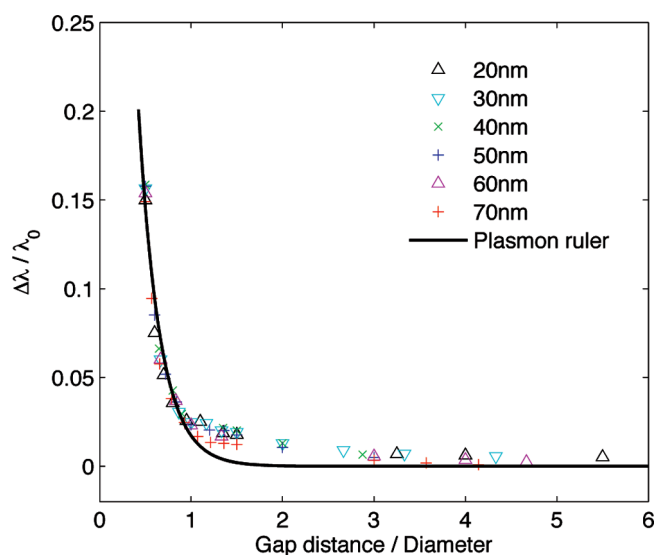


Figure 4. DDA results of scaled LSPR wavelength shift versus scaled gap distance for nanosphere diameters ranging from 20 to 70 nm. We find that these follow a universal trend that can be fitted to the plasmon ruler $y = a \exp[-(x - 0.414)/(\tau)]$, with the coupling strength $a = 0.21 \pm 0.02$ and the decay constant $\tau = 0.23 \pm 0.02$.

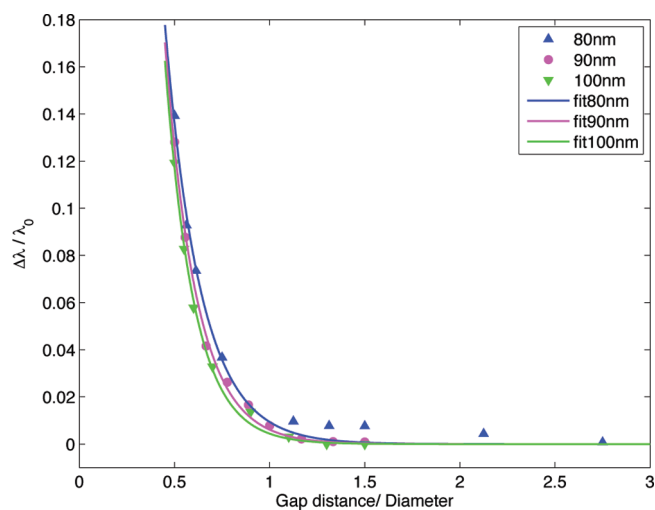


Figure 5. DDA results of scaled LSPR wavelength shift versus gap distance-to-diameter ratio for 80, 90, and 100 nm diameter nanospheres. We fit each data set to the plasmon ruler $y = a \exp[-(x - 0.414)/(\tau)]$ individually, obtaining the decay constants $\tau = 0.19, 0.17,$ and 0.15 , while the coupling strengths are very similar, $a = 0.22, 0.21,$ and 0.21 , respectively.

plot, whereas Figure 5 shows a similar plot, except containing only nanosphere diameters ranging from 80 to 100 nm. A similar fitting function as for the nanoparticle dimer case that was studied by Jain et al.¹ was utilized because both Figures 4 and 5 show that the LSPR wavelength shift decays rapidly with increasing nanosphere gap distance and reaches a near zero value if the nanosphere distance increases beyond a gap distance-to-diameter ratio of about 3. Because this behavior is similar to the dimer behavior reported by Jain et al.,¹ it can be approximated as an exponentially decaying function, which is known as a plasmon ruler equation, if the LSPR wavelength shifts $\Delta\lambda$ of the infinite,

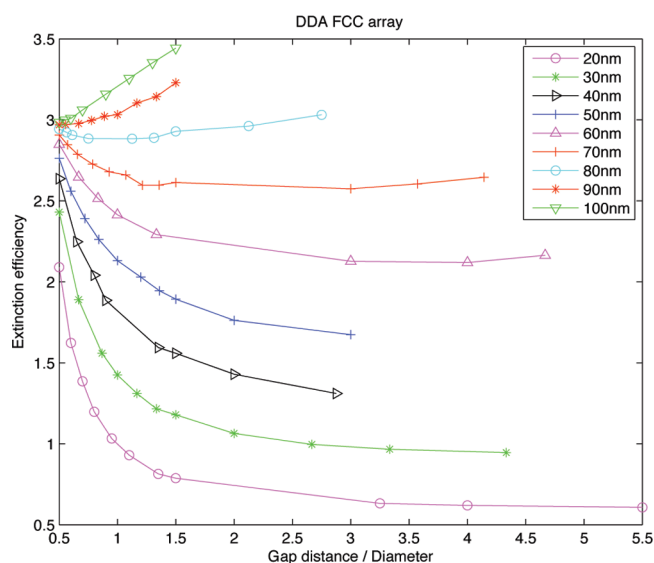


Figure 6. DDA results of extinction efficiency versus scaled gap distance for nanosphere diameters ranging from 20 to 100 nm.

periodic 2D array are scaled by the single sphere resonance wavelength λ_0 , and the gap distances T are scaled by the diameter D of the corresponding single sphere. Hence, the plasmon ruler equation we applied for fitting the data from both DDA (and the semianalytical CDA discussion in the next section) is

$$\frac{\Delta\lambda}{\lambda_0} = ae^{-\frac{x - 0.414}{\tau}} \quad (5)$$

where $x = T/D$. By fitting the data in Figure 4 for the 20–70 nm diameter nanospheres, we find a trend that appears to be independent of nanosphere diameter, where the decay constant $\tau = 0.23 \pm 0.02$ and the particle coupling strength $a = 0.21 \pm 0.02$.

We compare the value for the decay constant τ that is obtained for the infinite, periodic 2D array to the nanoparticle dimers that were previously reported in the literature. Specifically, Jain et al.¹ reported a decay constant $\tau = 0.23 \pm 0.03$ for gold nanodisk dimers using DDA calculations, whereas an experimental value of $\tau = 0.18 \pm 0.02$ was found for the same nanodisk dimers. Similarly, a decay constant of $\tau = 0.22$ was reported by Gunnarsson et al.⁶⁶ for silver nanodisk pairs. Thus, our results strongly suggest that 2D infinite periodic arrays of gold nanospheres with diameters smaller than a critical value of about 70 nm follow the same universal decay rule, in which the plasmon coupling strength decays exponentially with a decay length that is approximately 0.2 in units of particle size.

In contrast, Figure 5 shows the results for the 80, 90, and 100 nm diameter nanospheres, where the scaled LSPR wavelength shift for each diameter was fit individually. In doing so, we find that the decay constant decreases with increasing nanosphere diameter. Specifically, the decay constant τ decreases to a value of 0.15 for an infinite, periodic 2D array of 100 nm diameter gold nanospheres.

In addition to the size-dependent LSPR wavelength shift and plasmon ruler equation, we have also found that there is a size-dependent transition for the trend of the extinction efficiency, as shown in Figure 6. Specifically, the extinction efficiency increases as the nanosphere gap distance decreases for nanosphere diameters smaller than 70 nm, whereas a decrease in the extinction

efficiency with decreasing gap distance is found for nanosphere diameters larger than 70 nm. We will explain both the size-dependent trends in the LSPR wavelength shift and the extinction efficiency using the semianalytical CDA in the next section.

■ COMPARISON TO SEMIANALYTICAL COUPLED DIPOLE APPROXIMATION

Coupled Dipole Approximation—Theory. To assist in the analysis of the DDA results, we employ a semianalytical approach to analyze the far-field optical properties of metal nanosphere arrays based upon the coupled dipole approximation (CDA). As described by Zhao et al.,⁴⁴ the CDA is conceptually similar to the DDA, though with important differences. First, in the DDA, each sphere is discretized with a finite number of dipoles that have different polarizabilities, whose interactions lead to an exact representation of all higher-order (multipole) contributions to the LSPR. In contrast, in the CDA, each nanosphere has a homogeneous dipolar polarizability throughout the volume such that interactions between different nanospheres occur only at the dipolar level. The CDA was also utilized by Jain et al.¹ to assist in their interpretation of their nanoparticle dimer results, though both the size-dependent single sphere retardation effects of DD and RD and the structural retardation (see eq 8 below) were not accounted for.

To utilize the CDA, rather than using the near-field expression for a dipole, we must utilize its radiative counterpart to describe electric field effects beyond 100 nm distances, which also plays an important role in our infinite 2D array. The local field at the *i*th sphere can be expressed as the sum of the external field and the induced field due to all other dipoles in the 2D array as

$$\mathbf{E}_{\text{loc},i} = \mathbf{E}_{\text{inc}} + \sum_{j \neq i} \left(k^2 (\mathbf{n}_{ij} \times \mathbf{P}_j) \times \mathbf{n}_{ij} \frac{\exp(ikr_{ij})}{r_{ij}^3} + (3\mathbf{n}_{ij}(\mathbf{n}_{ij} \cdot \mathbf{P}_j) - \mathbf{P}_j) \left(\frac{1}{r_{ij}^3} - \frac{ik}{r_{ij}^2} \right) \exp(ikr_{ij}) \right) \quad (6)$$

where \mathbf{n}_{ij} is the unit vector pointing from the *i*th to the *j*th sphere and \mathbf{P}_j is the polarization for the *j*th sphere, which is defined as $\mathbf{P}_j = \alpha_{\text{sphere}} \mathbf{E}_{\text{loc},j}$. We assume that the 2D nanosphere array is infinite, the wave vector of the incident field is perpendicular to the plane containing the array, the polarization vector is parallel to the plane of the infinite 2D array and in the [100] direction, and that the local field at each sphere as well as the polarization of each sphere is identical. Therefore, eq 6 for our infinite 2D array simplifies to

$$\mathbf{E}_{\text{loc}} = \mathbf{E}_{\text{inc}} + S \cdot \alpha_{\text{sphere}} \mathbf{E}_{\text{loc}} \quad (7)$$

where the retarded dipole sum *S* is

$$S = \sum_{j \neq i} \left(k^2 \sin^2 \theta \frac{e^{(ikr_{ij})}}{r_{ij}} + (3 \cos^2 \theta - 1) \left(\frac{1}{r_{ij}^3} - \frac{ik}{r_{ij}^2} \right) e^{ikr_{ij}} \right) \quad (8)$$

We emphasize that *S* accounts for structural retardation effects via the geometric arrangement of the nanospheres due to the fact that it depends only on the distance r_{ij} between nanospheres. The effective polarizability of the infinite periodic 2D array is

then obtained as^{30,38}

$$\alpha_{\text{array}} = \frac{\alpha_{\text{sphere}}}{1 - S\alpha_{\text{sphere}}} \quad (9)$$

Because the CDA considers only dipolar interactions, and thus is most accurate for ultrasmall nanoparticle sizes at which the quasistatic approximation holds, we have accounted for finite size single sphere retardation effects, including DD and RD, to determine if these size effects become significant for the 2D periodic array with larger (70–100 nm) nanosphere diameters. We accomplished this by following the analytic work of Meier and Wokaun,⁵⁷ where the single sphere polarizability is described by a size-dependent function

$$\alpha_{\text{sphere}} = \frac{\epsilon - \epsilon_m}{(\epsilon + 2\epsilon_m) - (\epsilon - \epsilon_m)q^2 - (\epsilon - \epsilon_m)i^{2/3}q^3} a^3 \quad (10)$$

where *a* is the radius of the sphere and $q = ka$. The last two terms in the denominator are the size modifications of the quasistatic single sphere polarizability $\alpha = [(\epsilon - \epsilon_m)/(\epsilon + 2\epsilon_m)]a^3$.

Specifically, the term $-(\epsilon - \epsilon_m)q^2$ corresponds to DD, which accounts for the red shift of the single particle resonance wavelength that occurs for larger nanosphere diameters. The physical interpretation of DD is that, as the nanosphere diameter increases, so does the distance between the opposite charges of the induced dipole at each end of the nanosphere.⁶⁷ Because the restoring Coulombic force between the induced dipoles is proportional to $1/a^2$, the DD term contains a factor of q^2 . Thus, due to the decreased restoring force and thus increased polarization from DD, larger diameter nanospheres exhibit a reduced resonance frequency, resulting in the well-known red shifted LSPR wavelength with increasing nanosphere diameter.⁶¹

The $-(\epsilon - \epsilon_m)i^{2/3}q^3$ term accounts for RD, which causes broadening of the resonance peak and reduces the magnitude of the resonance for larger nanosphere diameters. The physical interpretation of RD is one in which the energy of the resonant electron oscillation, and thus the extinction efficiency, is reduced by radiative losses to photon scattering. Because scattering constitutes an increasingly large contribution to the optical extinction with increasing nanosphere diameter,⁶¹ the radiative (scattering) losses are captured in RD via the volume-dependent q^3 term. However, RD is not important for smaller nanospheres because the radiative losses are minimized due to the fact that the optical response is dominated by absorption, and not scattering, and is captured by the decrease of the nanosphere volume through the q^3 term. Thus, the size effects disappear and the polarization reduces to its quasistatic counterpart in the limit $k \rightarrow 0$.

Having defined all values needed to calculate α_{array} in eq 9, we can generate the extinction cross section as

$$C_{\text{ext}} = 4\pi k \text{Im}(\alpha_{\text{array}}) \quad (11)$$

In our present semianalytical comparison, the optical response of gold was approximated using the Drude–Lorentz model, with parameters from Hohenau and Krenn.⁶⁸ We applied this modified semianalytical model for different sphere sizes ranging from 20 to 100 nm, with tunable lattice spacing to compare against the obtained DDA results.

Coupled Dipole Approximation—Comparison to DDA. As previously discussed for the DDA, as shown in Figure 2, we found that the LSPR wavelength shift for the smallest gap distance of

0.5D (or center-to-center distance of 1.5D) increased with increasing nanosphere diameter until a critical diameter of about 50 nm was reached, after which a corresponding decrease was observed with increasing nanosphere diameter. Qualitatively similar results are also obtained using the CDA, as shown in Figure 7. As can be seen, the LSPR wavelength shift increases with increasing nanosphere diameter until the diameter becomes 70 nm; after that size, a clear decrease in the LSPR wavelength shift can be observed with increasing nanosphere diameter. In further comparing the DDA results in Figure 2 and the CDA results in Figure 7, it is clear that the CDA slightly underpredicts the LSPR wavelength shift for the same nanosphere diameter.

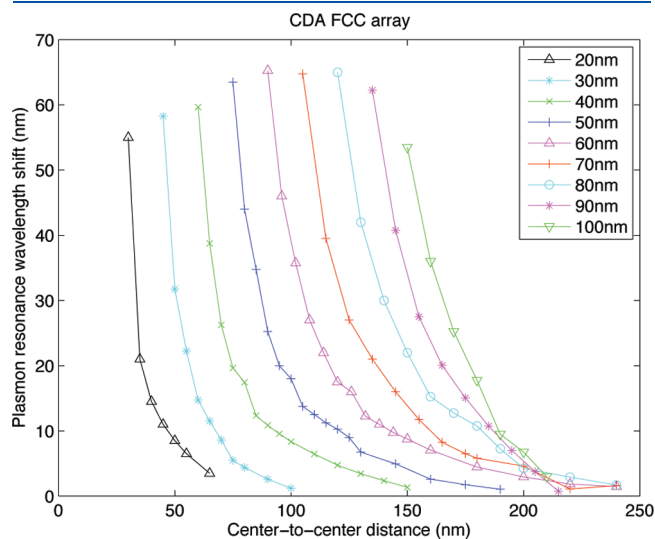


Figure 7. CDA results of LSPR wavelength shift versus gap distance for nanosphere diameters ranging from 20 to 100 nm. For the smallest center-to-center distance considered (1.5D), the wavelength shifts first increase and then decrease for nanosphere diameters larger than about 80 nm.

We also note the seemingly anomalous behavior with regards to the extinction maxima that was observed using the DDA. Specifically, it is well known that individual *fcc* metal nanospheres exhibit an increase in extinction efficiency with increasing diameter,⁶¹ up to a critical diameter. However, despite the fact that an LSPR red shift and peak broadening are observed for all nanosphere diameters (20–100 nm) with a decrease in gap distance, we find using the CDA, as shown in Figure 8, that the extinction efficiency decreases for decreasing gap distance for infinite, periodic 2D arrays for nanosphere diameters larger than about 70 nm, whereas it increases only for nanosphere diameters smaller than 70 nm. Again, the similarity between the CDA results in Figure 8a and the DDA results in Figure 6 is readily apparent.

Both of these unique results can be interpreted using the CDA, where it is known that the retarded array sum in eq 8 coupled with the modified single sphere polarizability in eq 10 contributes to both the shift of the LSPR wavelength and the line width with changes in the array spacing. To assist in the interpretation, we note that it was previously shown by Zhao et al.⁴⁴ that the real and imaginary parts of the retarded array sum S in eq 10 hold different physical meanings. Specifically, a positive real part leads to a red shift in the LSPR wavelength, whereas a negative real part results in a blue shift. Also, a positive imaginary part of S corresponds to a broadening of the LSPR line width, whereas a negative one corresponds to a narrowing of the line width. Thus, by comparing the difference between the real parts of $1/\alpha_{\text{sphere}}$ and S , we can determine the relative amount of the LSPR wavelength shift. Similarly, by comparing the difference between the imaginary parts of $1/\alpha_{\text{sphere}}$ and S , we can determine the variation in the extinction maxima, as shown in eq 11.

Therefore, we show in Tables 1–3 the retarded array sum, S , and modified single sphere polarizability, $1/\alpha_{\text{sphere}}$ for 20, 70, and 90 nm diameter 2D arrays, where all values were evaluated at the LSPR wavelength of the array for each size and gap distance. We will utilize these values below to explain the observed size dependence in both the LSPR wavelength shift and extinction

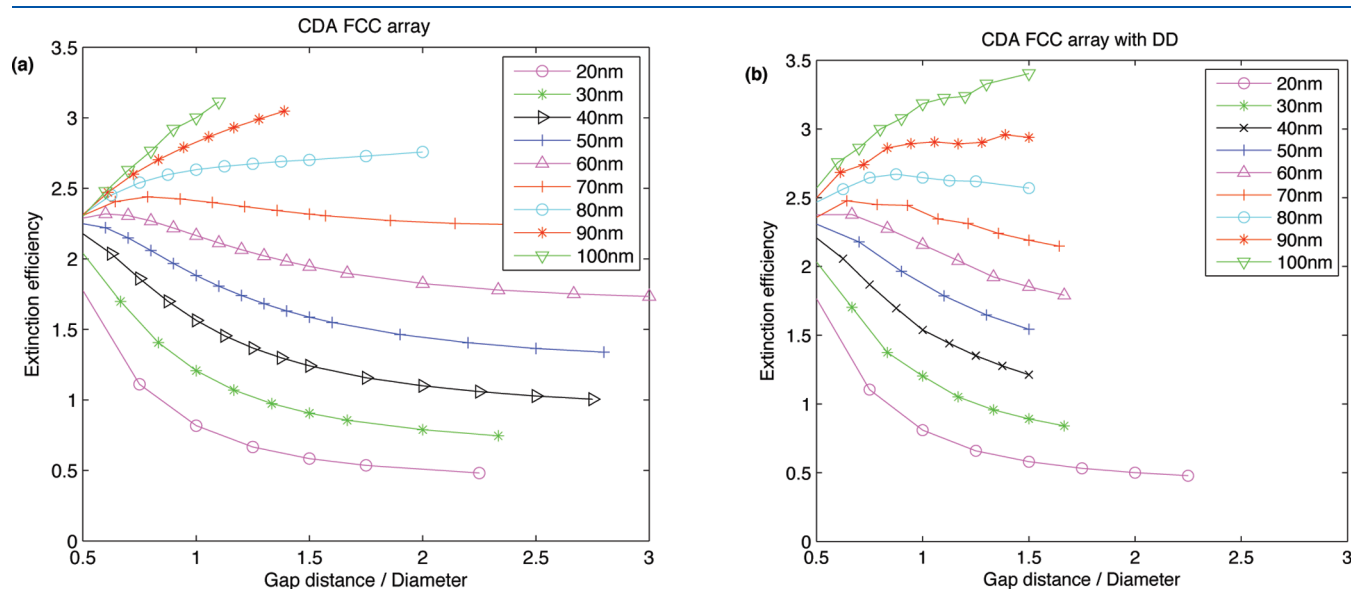


Figure 8. CDA results of extinction efficiency versus scaled gap distance for nanosphere diameters ranging from 20 to 100 nm: (a) including both DD and RD and (b) including DD only. The similarity of (b) to the DDA results in Figure 6 and the CDA results, including DD and RD, in (a) should be noted, indicating the dominant effect of DD in causing the size-dependent extinction that is observed.

Table 1. CDA Values for a 2D *fcc* Array with 20 nm Diameter Nanospheres Accounting for Both DD and RD

gap (nm)	S	$1/\alpha_{\text{sphere}}$	$1/\alpha_{\text{sphere}} - S$
10	4.4549 + 1.2466i	5.0257 - 0.5755i	0.5707 - 1.8221i
15	2.7278 + 0.9712i	4.2538 - 1.4812i	1.5260 - 2.4525i
30	0.9082 + 0.5212i	4.1600 - 2.1650i	3.2518 - 2.6862i

Table 2. CDA Values for a 2D *fcc* Array with 70 nm Diameter Nanospheres Accounting for Both DD and RD

gap (nm)	S	$1/\alpha_{\text{sphere}}$	$1/\alpha_{\text{sphere}} - S$
35	2.5967 + 4.9246i	2.5482 - 2.7436i	-0.0485 - 7.6682i
45	2.0411 + 3.6987i	3.4809 - 1.1049i	1.4398 - 4.8037i
65	0.8242 + 2.7306i	2.9367 - 1.6165i	2.1125 - 4.3471i

Table 3. CDA Values for a 2D *fcc* Array with 90 nm Diameter Nanospheres Accounting for Both DD and RD

gap (nm)	S	$1/\alpha_{\text{sphere}}$	$1/\alpha_{\text{sphere}} - S$
45	2.1831 + 5.3006i	3.3568 - 1.0791i	1.1737 - 6.3797i
65	0.6478 + 4.1207i	2.3797 - 1.5922i	1.7319 - 5.7129i
75	0.1803 + 3.5935i	2.1187 - 1.7915i	1.9384 - 5.3805i

maxima, similar to the approach previously taken by Zhao et al.⁴⁴ and Haynes et al.³⁸

As the gap distance between the nanospheres decreases, we find that both the real and the imaginary parts of the retarded 2D array sum S in eq 8 and Tables 1–3 become increasingly positive for all nanosphere diameters, which indicates both an LSPR red shift and a broadening of the resonance peak. Thus, the CDA correctly predicts both the LSPR red shift and the peak broadening for all nanosphere diameters with a decrease in gap distance.

If we compare the values of both S and α_{sphere} at the resonance wavelength of each specific array arrangement, we can obtain the far-field optical properties, such as the extinction efficiency, at the particular resonance wavelength. This point should be emphasized, because later in this section after analyzing the extinction properties, we will be calculating S and α_{sphere} at different resonance wavelengths in order to understand the origins of the size-dependent wavelength shifts.

To explain the size dependence of the extinction behavior of arrays using the CDA, we note that extinction represents the amount of light removed from the incident beam by interference between the incident and forward scattered light, which depends on both the retarded dipole sum S and the single sphere polarizability α_{sphere} . For the 2D array, the peak extinction efficiency is proportional to $(1)/(|\text{Im}(1/\alpha_{\text{sphere}} - S)|)$, where the $|\text{Im}(1/\alpha_{\text{sphere}} - S)|$ term is shown in Tables 1–3. Again, we emphasize that the values for each row in the three tables are calculated at the same λ_{array} , the resonance wavelength of the array, in order to compare the extinction properties for arrays with the same nanosphere size, but different gap distances. As can be seen in Table 1 for the 20 nm diameter 2D array, a decrease in $|\text{Im}(1/\alpha_{\text{sphere}} - S)|$ is observed with decreasing gap distance, which results in an increased value of $(1)/(|\text{Im}(1/\alpha_{\text{sphere}} - S)|)$, and thus an increase in the extinction efficiency. In contrast, for the 70 and 90 nm diameter 2D arrays in Tables 2 and 3, an

Table 4. CDA Values for a 2D *fcc* Array for Nanosphere Diameters Ranging from 20 to 100 nm with a 0.5D Gap Distance

diameter (nm)	$S (\lambda_{\text{array}})$	$(1/\alpha_{\text{sphere}}) (\lambda_{\text{sphere}})$	$ \text{Re}((1/\alpha_{\text{sphere}}) - S) $
20	4.4549 + 1.2466i	4.3324 - 2.6983i	0.1225
30	4.3322 + 1.8813i	4.1467 - 2.6985i	0.1855
40	4.1186 + 2.5004i	3.8783 - 2.7113i	0.2403
50	3.8714 + 3.1162i	3.5139 - 2.7134i	0.3575
60	3.5416 + 3.7055i	3.0678 - 2.7270i	0.4738
70	3.1372 + 4.2764i	2.5473 - 2.7109i	0.5899
80	2.7218 + 4.8172i	1.9914 - 2.6789i	0.7304
90	2.1831 + 5.3006i	1.4627 - 2.6027i	0.7204
100	1.5939 + 5.7842i	1.0291 - 2.5234i	0.5604

increase in $|\text{Im}(1/\alpha_{\text{sphere}} - S)|$ is observed for decreasing gap distance, which leads to a decrease of $(1)/(|\text{Im}(1/\alpha_{\text{sphere}} - S)|)$, and the observed decrease in extinction efficiency.

To explain the observed decrease in the LSPR wavelength shift for increasing nanosphere diameters using the CDA, we recall that a more positive real part of the retarded sum S results in a larger red shift of the LSPR wavelength. Thus, to explain the observation that, with increasing nanosphere diameter, the LSPR wavelength shift first increases for smaller nanosphere diameters and then begins to decrease for nanosphere diameters larger than about 70 nm, we compare in Table 4 the value of the retarded dipole sum S at the LSPR wavelength λ_{array} for each array to the value of the single sphere polarizability at the single sphere LSPR wavelength λ_0 , in order to determine the amount of the array LSPR wavelength shifts with respect to each single sphere LSPR wavelength shift. This is also important as this is how the plasmon ruler is calculated; see eq 5. In this case, $|\text{Re}(1/\alpha_{\text{sphere}} - S)|$ corresponds to the relative LSPR wavelength shift between the array and the single sphere $\Delta\lambda = \lambda - \lambda_0$. As shown in Table 4, the value of $|\text{Re}(1/\alpha_{\text{sphere}} - S)|$ increases from 20 to 70 nm but then decreases for larger nanosphere diameters, which agrees well with the size-dependent LSPR wavelength shifts seen in Figures 2 and 7.

Having established that the CDA with DD and RD can capture the observed size dependence in both the LSPR wavelength shift and the extinction efficiency, we delineate the specific single sphere retardation effect that is most critical. We determined this by using the CDA with the single sphere polarizability α_{sphere} calculated in four different forms: the quasistatic polarizability, RD only, DD only, and both RD and DD. The most relevant result is shown in Figure 8b for the DD-only case, where a striking similarity to both the CDA result in Figure 8a accounting for both DD and RD and the DDA results in Figure 6 can be observed. Furthermore, we show in Figure 9 the CDA results for the scaled LSPR wavelength shift as a function of scaled gap distance while accounting for DD only. It is clear that, in accounting for DD-related single sphere retardation effects in the CDA calculation, the size-dependent deviation from the plasmon ruler equation that was previously observed for the DDA in Figure 3 is replicated.

Figure 10 demonstrates that, if the nanospheres with diameters ranging from 20 to 70 nm are combined into a single universal plot, the CDA, including both DD and RD, predicts a plasmon ruler equation with a decay constant of $\tau = 0.42$ and magnitude of 0.14. Furthermore, we have also fit the 20–70 nm

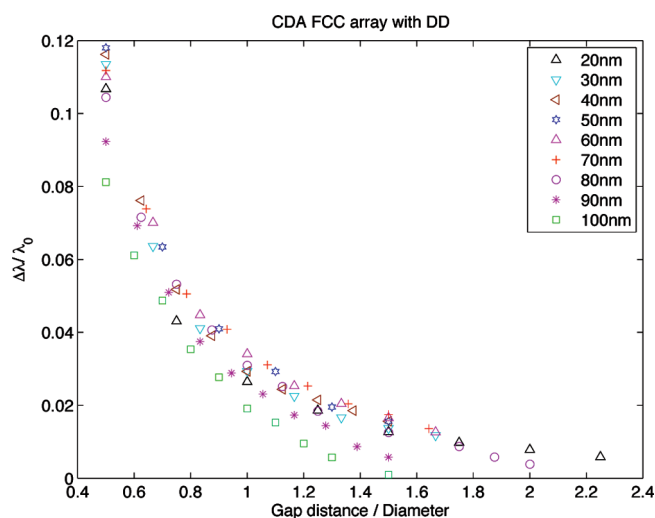


Figure 9. CDA results of scaled LSPR wavelength shift versus scaled gap distance for nanosphere diameters from 20 to 100 nm accounting for the DD-related retardation effect only. It is clear that the size-dependent deviation from the universal plasmon ruler that was previously observed in Figure 3 using the DDA is also observed here.

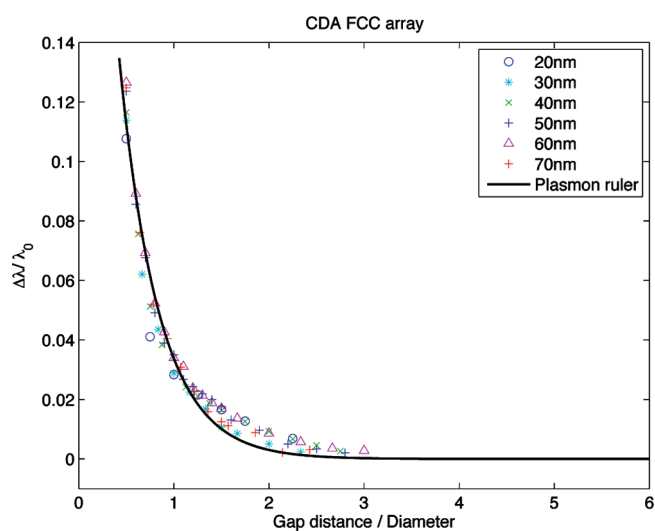


Figure 10. CDA results of scaled LSPR wavelength shift versus scaled gap distance for nanosphere diameters ranging from 20 to 70 nm. The data points are fitted together to the plasmon ruler $y = a \exp[-(x - 0.414)/(\tau)]$, with decay constant $\tau = 0.42 \pm 0.02$ and magnitude $a = 0.14 \pm 0.01$.

data obtained using DD-only together, resulting in a decay constant $\tau = 0.42$, which is the same as obtained using the CDA with both DD and RD, which implies that the single sphere DD effects coupled with structural retardation are the dominant effects in causing the observed size dependence of the plasmon ruler equation. The fact that the CDA plasmon ruler constants differ from that predicted from the DDA is not surprising, considering that higher-order multipole effects are neglected, and reflects the fact that the CDA underestimates the coupling strength between the nanospheres at small distances.¹ We note that similar values for the decay constant and magnitude were also found by Jain et al.¹ using a quasistatic analytical method for the nanodisc dimer case.

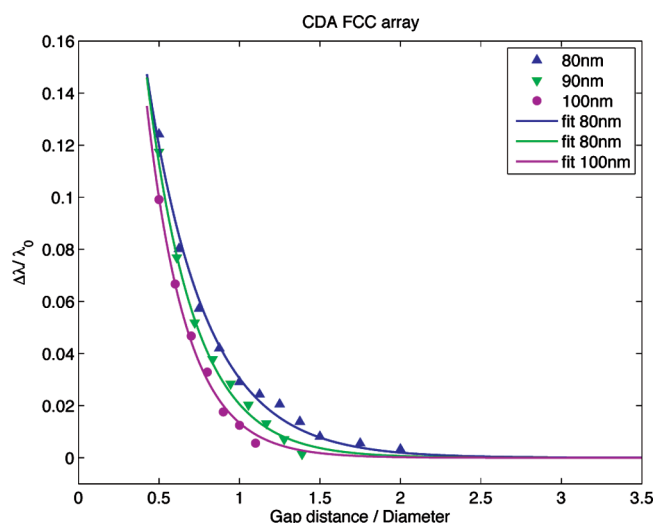


Figure 11. CDA results of scaled LSPR wavelength shift versus scaled gap distance and fitted curves for nanosphere diameters of 80, 90, and 100 nm. We fit each data set to the plasmon ruler $y = a \exp[-(x - 0.414)/(\tau)]$ individually, obtaining the decay constants $\tau = 0.37, 0.29$, and 0.25 , with similar magnitudes $a = 0.15, 0.16$, and 0.14 , respectively.

We also demonstrate the decrease in decay constants τ for the larger diameter nanospheres as predicted using the CDA in Figure 11. There, a clear decrease in the decay constant from $\tau = 0.42$ in the universal case for the 20–70 nm diameters to $\tau = 0.25$ for the 100 nm diameter case is observed. This is in good agreement with the DDA results, where, for the CDA, the decay constant for the 100 nm diameter case decreases 40% as compared with the universal decay constant, whereas in the DDA, the decrease for the 100 nm diameter case is 33% as compared with the universal decay constant. The agreement between CDA and DDA is encouraging and suggests that the small difference in the two results from the fact that multipole interactions are neglected in the CDA. However, this demonstrates that, even considering only dipolar interactions, the CDA is an effective methodology to gain physical insights into the optical properties of 2D nanosphere arrays.

Finally, we also discuss the implications of DD-driven retardation effects on the functional form of the plasmon ruler. Specifically, Jain and El-Sayed have recently noted in a recent review on plasmonic coupling⁶⁹ that an observable discrepancy between the DDA and experimental results and the exponential fitting function exists in the gap distance/diameter (T/D) range of about 1–2 for nanoparticle dimers. This discrepancy is also observed for our 2D array cases, as seen in the DDA calculations for the 20–70 nm diameter nanospheres in Figure 4. In contrast, as shown in Figure 5 for the larger sphere sizes of 80–100 nm, as the nanosphere diameter increases, the plasmon coupling appears to converge toward an exponentially decaying value and is well-fitted by the exponential function for the entire T/D range.

The same trend is observed using the CDA calculations accounting for DD, as can be seen in Figure 10 for the 20–70 nm diameter range, in which the deviation from the exponential function for the T/D range of 1–2 is observed, and in Figure 11 for the 80–100 nm diameter range, where the increasing agreement with the exponential fitting function is again observed. Therefore, we conclude that the discrepancy between the DDA results and the exponential fitting function in the T/D range of 1–2 can be attributed to the effects

of DD-driven retardation. Mathematically, this occurs because, while in the quasistatic approximation, the plasmon ruler has a $1/(T/D)^3$ dependence, the addition of DD adds an additional factor of $1/(T^3/D)$ dependence, which causes the plasmon coupling strength to decay more quickly as compared with the purely quasistatic case, and thus leads to better agreement with the exponential fitting function.

Comparison Between Dimer and Periodic 2D Array. An important question that we address now is, why is a size dependence in the plasmon ruler predicted for the infinite, periodic 2D array when it was not reported for the dimer case by Jain et al.¹ To do so, we utilize the same semianalytical CDA approach summarized previously for the 2D array. Specifically, we account for single sphere retardation effects with appropriate modifications for the dimer geometry by considering structural retardation and near-field coupling effects to give the effective dimer polarizability α_{dimer} similar to that in eq 9 for the 2D array

$$\alpha_{\text{dimer}} = \frac{1}{\frac{1}{\alpha_{\text{sphere}}} - S} \quad (12)$$

where parallel polarization of the incident light is considered. We note that, in Jain et al.,¹ the dimer structure sum S is

$$S_{\text{Jain}} = \frac{2}{r_{ij}^3} \quad (13)$$

whereas in the present analysis, the dimer structure sum S is

$$S_{\text{dimer}} = 2 \left(\frac{1 - ikr_{ij}}{r_{ij}^3} \right) e^{ikr_{ij}} \quad (14)$$

where r_{ij} is the center-to-center distance between the two nanospheres. The difference between the two dimer structure sums occurs because of the quasistatic approximation utilized by Jain et al.,¹ which neglects the structural retardation that occurs due to the oscillatory $e^{ikr_{ij}}$ term.

Our analytical CDA results for the dimer show a decay constant τ of about 0.40 for nanosphere diameters between 20 and 70 nm, which is in agreement with that previously reported using the quasistatic CDA by Jain et al.¹ However, for dimers with nanosphere diameters larger than 70 nm, we observe a weak size dependence of the decay constant of the plasmon ruler equation for dimers that is similar to that observed for the 2D arrays. Specifically, the decay constant for the dimer decreases slightly from 0.44 (70 nm diameter) to 0.37 (100 nm diameter) for the dimer case; this is in contrast to the much larger drop from 0.39 (70 nm diameter) to 0.25 (100 nm diameter) that was predicted using the CDA for the 2D array case.

The weaker size dependence of the dimer plasmon ruler as compared to the 2D array case can be explained as follows. First, as noted by Zhao et al.,⁴⁴ the far-field interaction term, or the $1/r_{ij}$ term in eq 8, is zero for the dimer case as all angles θ are zero. However, this term does not disappear for the array case and is thus critical for predicting the size-dependent plasmon ruler equation for 2D arrays.

Second, in analyzing the retarded sum S_{dimer} in eq 14 for nanosphere diameters between 20 and 100 nm, the imaginary part is found to be essentially independent of the center-to-center distance r_{ij} and is small compared to the real part of S_{dimer} even for nanosphere diameters up to 100 nm. This is relevant because the imaginary part of S_{dimer} is known to control the width and

intensity of the plasmon resonance. If this is essentially size-independent, then it suggests that, for the dimer analysis, it is reasonably accurate to take $kd \rightarrow 0$, which would cause $S_{\text{dimer}} = S_{\text{Jain}}$, and implies that structural retardation effects, which are dependent upon the geometric arrangement of the nanospheres and are mathematically represented by the $e^{ikr_{ij}}$ terms, are relatively unimportant for the dimer case as compared to the 2D array case. Therefore, although this would cause the structure sum S to be the same between the current work and that of Jain et al.,¹ the size dependence of the plasmon ruler in the present work for dimers primarily arises because the single sphere polarizability α_{sphere} in eq 12 accounts for both DD and RD, which were not considered by Jain et al.¹

Having analyzed the causes of the size dependence of the plasmon ruler for both 2D arrays and the dimer case, we discuss the generality of the critical 70 nm diameter for the onset of the size dependence. Specifically, the critical 70 nm diameter should be a value that is specific to gold, whereas other metals of interest, such as silver, will have a different critical transition diameter for the manifestation of a size-dependent plasmon ruler. This is because, for both arrays and dimers, the critical diameter is related to α_{sphere} , which depends on both the material dielectric function and the nanosphere diameter.

Discussion and Experimental Comparison. We now place our results in the context of available experimental data on the optical properties of 2D nanoparticle arrays, and in doing so, we first note that we were unable to find any experimental studies that measured or determined the plasmon ruler for 2D arrays. One relevant experimental study is that performed by Haynes et al.,³⁸ who studied the optical properties of gold and silver cylinders and prisms in 2D hexagonal and square arrays, where the nanoparticles were all about 200 nm in diameter or size. For the gold nanoparticles, evidence of the decrease in extinction efficiency with decreasing gap distance was observed in that work. Interestingly, the authors also reported theoretical calculations based on a retardation-corrected CDA model very similar to the one discussed in the present work, which led to predictions of a gap distance-dependent red shift for smaller gap distances. However, this red shift was not observed experimentally, which the authors attributed to either deficiencies in the CDA model or, alternatively, because the size of the nanoparticles considered (200 nm) precluded them from achieving the small gap distances at which the red shift was predicted theoretically. We should note that, because we have performed DDA calculations in which the size dependence was observed for both the extinction and the plasmon ruler, the shortcomings of the CDA model do not appear to explain the discrepancy between theory and experiment.

In addition to the work of Haynes et al.,³⁸ we also note the more recent work of Kinnan and Chumanov,³⁹ who studied 2D arrays of somewhat randomly oriented silver nanoparticles with sizes ranging from about 50 to 300 nm. In that work, a similar size-dependent decrease in the extinction efficiency for smaller nanoparticle separations was also observed for nanoparticle sizes exceeding about 90 nm. Furthermore, a very slight red shift with decreasing interparticle distance was also observed in that work. However, the wavelength shifts are fairly small, and thus the size dependence of the plasmon ruler cannot be definitively inferred or ruled out from this experimental data.

Finally, we note in the original work by Jain et al. that a direct comparison to experiment was performed for three nanodisc diameters, 48, 64, and 86 nm, where no size dependence of the plasmon ruler was reported either theoretically or experimentally.

One possible reason that the size dependence was not reported by Jain et al.¹ in their DDA calculations was because they considered only three nanodisc diameters, 48, 64, and 86 nm, such that multiple large sphere sizes greater than 70 nm, which would be needed to observe the size dependence, were not considered. In addition, the analytical CDA model in Jain et al.¹ assumed that $kd \rightarrow 0$ and was based on the quasistatic approximation neglecting DD, RD, and structural retardation; therefore, no size dependence of the decay length was observed in their work. However, in extending their work to plasmon rulers for metal nanostructures of complex geometries⁷⁰ and trimers, it was noted that electromagnetic retardation effects on the universal plasmon ruler, which could be critical for larger nanoparticle sizes, have not been considered.

Overall, the current experimental data validate the current predictions regarding the size-dependent extinction behavior, though a similar experimental validation of the size-dependent plasmon ruler has not yet been reported.

Implications for Other Infinite, Periodic 2D Arrangements of Nanospheres. We close by discussing the implications of the

above findings based on the CDA on the size- and gap-dependent optical response of other, infinite periodic 2D arrangements of gold nanospheres, including a hexagonal arrangement of nanospheres and a simple cubic arrangement of nanospheres. The universal plasmon ruler fits for both array geometries are shown in Figure 12. There, we find that the decay constants are similar to, though not identical to, that exhibited by the $\{100\}$ *fcc* in Figure 10, where the simple cubic array shows the largest decay constant, but the smallest magnitude; the hexagonal array shows a decay constant that is also larger than the $\{100\}$ *fcc* case, but with a significantly larger magnitude. The variations in the coupling magnitudes are intuitive, as a single nanosphere in the hexagonal arrangement can interact with the most nearest-neighbor spheres, whereas a nanosphere in a simple cubic arrangement can interact with the smallest number of nearest-neighbor spheres.

The size and distance-dependent extinction efficiencies are shown for the 2D arrangements in Figure 13. There, it is again observed that the 70 nm diameter is the critical diameter; for larger diameters, the anomalous decrease in extinction efficiency

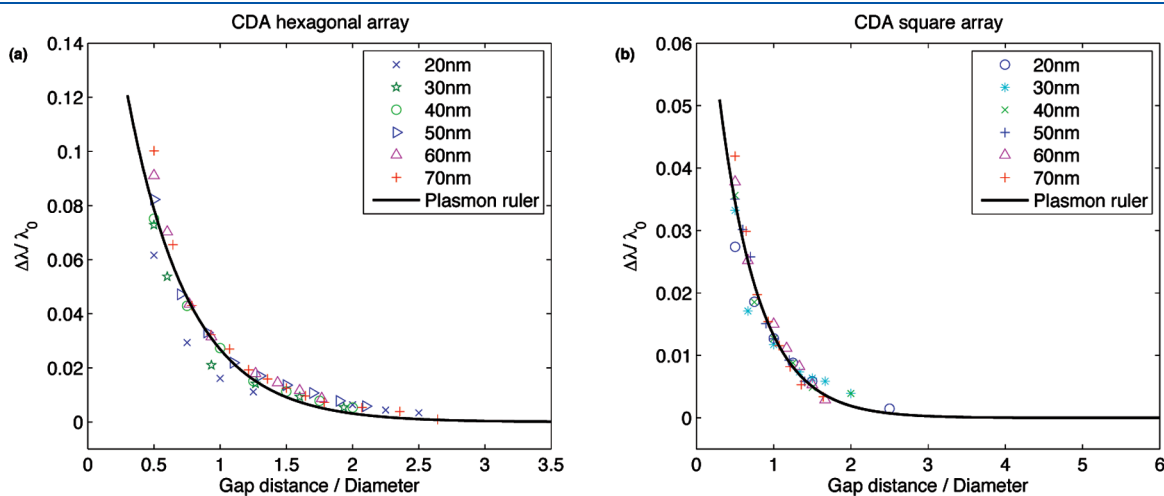


Figure 12. CDA results of scaled LSPR wavelength shift versus scaled gap distance for an infinite, periodic 2D array with nanosphere diameters ranging from 20 to 80 nm arranged in a (a) hexagonal and (b) simple cubic lattice structure. Both sets of data were fit to the plasmon ruler $y = a \exp -x/\tau$, resulting in decay constants $\tau_{\text{hex}} = 0.47$ and $\tau_{\text{sc}} = 0.51$ and magnitudes $a_{\text{hex}} = 0.23$ and $a_{\text{sc}} = 0.09$.

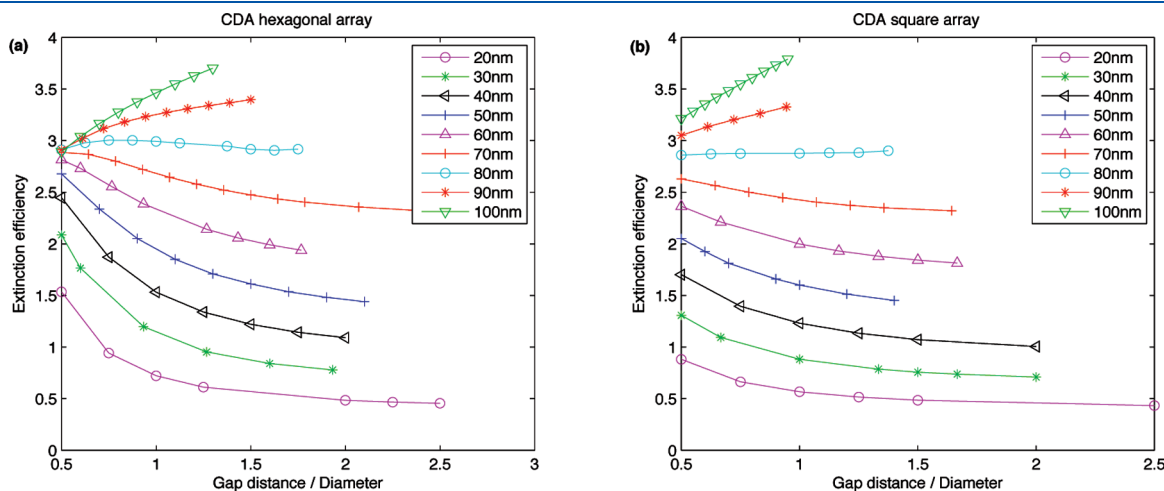


Figure 13. CDA results of extinction efficiency versus scaled gap distance for nanosphere diameters ranging from 20 to 100 nm arranged in a (a) hexagonal and (b) simple cubic lattice structure.

with decreasing gap distance is observed, using the CDA, for the three 2D infinite, periodic arrangements of nanospheres. Overall, this suggests that the size-dependent extinction maxima and LSPR wavelength shifts are general features that will be observed for infinite 2D, periodic arrangements of gold nanospheres.

CONCLUSIONS

In conclusion, we have presented a systematic study using the discrete dipole approximation of the far-field optical response of infinite, periodic 2D arrays of gold nanospheres with diameters ranging from 20 to 100 nm. In doing so, we have determined that, for nanosphere diameters smaller than about 70 nm, the arrays follow the universal plasmon ruler equation previously described by Jain et al.¹ for nanodisc dimers. However, for 2D arrays with nanosphere diameters larger than about 70 nm, a deviation from the universal plasmon ruler behavior and a decrease in extinction efficiency with decreasing gap distance is observed. Both of these anomalous size-dependent optical responses can be interpreted by including dynamic depolarization effects within a semianalytical coupled dipole approximation that also accounts for structural retardation due to the geometric arrangement of the nanospheres. The semianalytical approach was extended to examine the reasons why such a size-dependent plasmon ruler has not been reported for nanoparticle dimers. We found that this is because structural arrangement retardation effects, while still operant for nanoparticle dimers, are significantly reduced as compared to the 2D array case, thus leading to a substantial reduction of the size-dependent retardation effects as compared to the 2D array case. Finally, we have found that previously observed deviations from the exponential plasmon ruler fitting function in the gap distance-to-diameter range of 1–2 can be attributed to retardation effects arising from dynamic depolarization.

Our results have important implications for optical sensing and detection applications using periodic 2D arrays of gold nanoparticles. In particular, the value of a universal plasmon ruler is its implication that utilization of larger diameter nanospheres in the periodic 2D array will enlarge the sensing range in a manner that is proportional to the nanosphere diameter. However, our results place an upper bound on the extent to which nanoparticle sizes can be increased in order to increase the range of the plasmon ruler.¹ Overall, our results should enable size-dependent estimates of the interparticle separation in arrays of infinite, two-dimensional nanosphere arrays used in biodetection applications from the shift of the localized surface plasmon resonance wavelength that is observed experimentally.⁵¹

AUTHOR INFORMATION

Corresponding Author

*E-mail: parkhs@bu.edu.

ACKNOWLEDGMENT

Both authors acknowledge NSF grant number CMMI-0750395 in support of this research. Both authors also acknowledge the valuable comments of the two anonymous reviewers.

REFERENCES

(1) Jain, P. K.; Huang, W.; El-Sayed, M. A. *Nano Lett.* **2007**, *7*, 2080–2088.

- (2) Ozbay, E. *Science* **2006**, *311*, 189–193.
- (3) Sambles, J. R.; Bradbery, G. W.; Yang, F. *Contemp. Phys.* **1991**, *32*, 173–183.
- (4) Barnes, W. L.; Dereux, A.; Ebbeson, T. W. *Nature* **2003**, *424*, 824–830.
- (5) Nie, S.; Emory, S. R. *Science* **1997**, *275*, 1102–1106.
- (6) Hao, E.; Schatz, G. C. *J. Chem. Phys.* **2004**, *120*, 357–366.
- (7) Kneipp, K.; Moskovits, M.; Kneipp, H. E. *Surface-Enhanced Raman Scattering*; Springer: New York, 2006.
- (8) Kelly, K. L.; Coronado, E.; Zhao, L. L.; Schatz, G. C. *J. Phys. Chem. B* **2003**, *107*, 668–677.
- (9) Link, S.; El-Sayed, M. A. *J. Phys. Chem. B* **1999**, *103*, 8410–8426.
- (10) Lee, K.-S.; El-Sayed, M. A. *J. Phys. Chem. B* **2005**, *109*, 20331–20338.
- (11) Raschke, G.; Brogl, S.; Susha, A. S.; Rogach, A. L.; Klar, T. A.; Feldmann, J.; Fierres, B.; Petkov, N.; Bein, T.; Nichtl, A.; Kurzinger, K. *Nano Lett.* **2004**, *4*, 1853–1857.
- (12) Sokolov, K.; Follen, M.; Aaron, J.; Pavlova, I.; Malpica, A.; Lotan, R.; Richards-Kortum, R. *Cancer Res.* **2003**, *63*, 1999–2004.
- (13) El-Sayed, I. H.; Huang, X.; El-Sayed, M. A. *Nano Lett.* **2005**, *5*, 829–834.
- (14) Mock, J. J.; Oldenburg, S. J.; Smith, D. R.; Schultz, D. A.; Schultz, S. *Nano Lett.* **2002**, *2*, 465–469.
- (15) Anker, J. N.; Hall, W. P.; Lyandres, O.; Shah, N. C.; Zhao, J.; Duynes, R. P. V. *Nat. Mater.* **2008**, *7*, 442–453.
- (16) Brongersma, M. L.; Hartman, J. W.; Atwater, H. A. *Phys. Rev. B* **2000**, *62*, R16356–R16359.
- (17) Maier, S. A.; Brongersma, M. L.; Kik, P. G.; Meltzer, S.; Requicha, A. A. G.; Atwater, H. A. *Adv. Mater.* **2001**, *13*, 1501–1505.
- (18) Hirsch, L. R.; Stafford, R. J.; Bankson, J. A.; Sershen, S. R.; Rivera, B.; Price, R. E.; Hazle, J. D.; Halas, N. J.; West, J. L. *Proc. Natl. Acad. Sci. U.S.A.* **2003**, *100*, 13549–13554.
- (19) Hirsch, L. R.; Gobin, A. M.; Lowery, A. R.; Tam, F.; Drezek, R. A.; Halas, N. J.; West, J. L. *Ann. Biomed. Eng.* **2006**, *34*, 15–22.
- (20) Huang, X.; El-Sayed, I. H.; Qian, W.; El-Sayed, M. A. *J. Am. Chem. Soc.* **2006**, *128*, 2115–2120.
- (21) Haynes, C. L.; Duynes, R. P. V. *J. Phys. Chem. B* **2001**, *105*, 5599–5611.
- (22) Tao, A.; Sinsermsuksakul, P.; Yang, P. *Nat. Nanotechnol.* **2007**, *2*, 435–440.
- (23) Genov, D. A.; Sarychev, A. K.; Shalaev, V. M.; Wei, A. *Nano Lett.* **2004**, *4*, 153–158.
- (24) Xu, H.; Aizpurua, J.; Kall, M.; Apell, P. *Phys. Rev. E* **2000**, *62*, 4318–4324.
- (25) Kneipp, K.; Wang, Y.; Kneipp, H.; Perelman, L. T.; Itzkan, I.; Dasari, R. R.; Feld, M. S. *Phys. Rev. Lett.* **1997**, *78*, 1667–1670.
- (26) Tan, S. J.; Campolongo, M. J.; Luo, D.; Cheng, W. *Nat. Nanotechnol.* **2011**, *6*, 268–276.
- (27) Liu, N.; Hentschel, M.; Weiss, T.; Alivisatos, A. P.; Giessen, H. *Science* **2011**, *332*, 1407–1410.
- (28) Acimovic, S. S.; Kreuzer, M. P.; Gonzales, M. U.; Quidant, R. *ACS Nano* **2009**, *3*, 1231–1237.
- (29) Atay, T.; Song, J.-H.; Nurmikko, A. V. *Nano Lett.* **2004**, *4*, 1627–1631.
- (30) Auguie, B.; Barnes, W. L. *Phys. Rev. Lett.* **2010**, *101*, 143902.
- (31) Jiang, J.; Bosnick, K.; Maillard, M.; Brus, L. *J. Phys. Chem. B* **2003**, *107*, 9964–9972.
- (32) Kravets, V. G.; Schedin, F.; Grigorenko, A. N. *Phys. Rev. Lett.* **2008**, *101*, 087403.
- (33) Maier, S. A.; Brongersma, M. L.; Kik, P. G.; Atwater, H. A. *Phys. Rev. B* **2002**, *65*, 193408.
- (34) Rechberger, W.; Hohenau, A.; Leitner, A.; Krenn, J. R.; Lamprecht, B.; Aussenegg, F. R. *Opt. Commun.* **2003**, *220*, 137–141.
- (35) Su, K.-H.; Wei, Q.-H.; Zhang, X.; Mock, J. J.; Smith, D. R.; Schultz, S. *Nano Lett.* **2003**, *3*, 1087–1090.
- (36) Talley, C. E.; Jackson, J. B.; Oubre, C.; Grady, N. K.; Hollars, C. W.; Lane, S. M.; Huser, T. R.; Nordlander, P.; Halas, N. J. *Nano Lett.* **2005**, *5*, 1569–1574.

- (37) Wei, Q.-H.; Su, K.-H.; Durant, S.; Zhang, X. *Nano Lett.* **2004**, *4*, 1067–1071.
- (38) Haynes, C. L.; McFarland, A. D.; Zhao, L. L.; Duyne, R. P. V.; Schatz, G. C.; Gunnarsson, L.; Prikulis, J.; Kasemo, B.; Käll, M. *J. Phys. Chem. B* **2003**, *107*, 7337–7342.
- (39) Kinnan, M. K.; Chumanov, G. *J. Phys. Chem. C* **2010**, *114*, 7496–7501.
- (40) Aizpurua, J.; Bryant, G. W.; Richter, L. J.; de Abajo, F. J. G.; Kelley, B. K.; Mallouk, T. *Phys. Rev. B* **2005**, *71*, 235420.
- (41) Oubre, C.; Nordlander, P. *J. Phys. Chem. B* **2005**, *109*, 10042–10051.
- (42) Romero, I.; Aizpurua, J.; Bryant, G. W.; de Abajo, F. J. G. *Opt. Express* **2006**, *14*, 9988–9999.
- (43) Xu, H.; Käll, M. *Phys. Rev. Lett.* **2002**, *89*, 246802.
- (44) Zhao, L.; Kelly, K. L.; Schatz, G. C. *J. Phys. Chem. B* **2003**, *107*, 7343–7350.
- (45) Zou, S.; Janel, N.; Schatz, G. C. *J. Chem. Phys.* **2004**, *120*, 10871–10875.
- (46) Zou, S.; Schatz, G. C. *J. Chem. Phys.* **2004**, *121*, 12606–12612.
- (47) Tserkezis, C.; Papanikolaou, N.; Almpanis, E.; Stefanou, N. *Phys. Rev. B* **2009**, *80*, 125124.
- (48) Russier, V.; Pileni, M. P. *Surf. Sci.* **1999**, *425*, 313–325.
- (49) Dahmen, C.; Schmidt, B.; von Plessen, G. *Nano Lett.* **2007**, *7*, 318–322.
- (50) Sonnichsen, C.; Reinhard, B. M.; Liphardt, J.; Alivisatos, A. P. *Nat. Biotechnol.* **2005**, *23*, 741–745.
- (51) Reinhard, B. M.; Siu, M.; Agarwal, H.; Alivisatos, A. P.; Liphardt, J. *Phys. Rev. B* **2005**, *76*, 085420.
- (52) Cole, R. M.; Mahajan, S.; Baumberg, J. J. *Appl. Phys. Lett.* **2009**, *95*, 154103.
- (53) Olcum, S.; Kocabas, A.; Ertas, G.; Atalar, A.; Aydinli, A. *Opt. Express* **2009**, *17*, 8542–8547.
- (54) Sannomiya, T.; Hafner, C.; Voros, J. *Opt. Lett.* **2009**, *34*, 2009–2011.
- (55) Purcell, E. M.; Pennypacker, C. R. *Astrophys. J.* **1973**, *1986*, 705–714.
- (56) Draine, B. T.; Flatau, P. J. <http://arxiv.org/abs/0809.0337>, 2008.
- (57) Meier, M.; Wokaun, A. *Opt. Lett.* **1983**, *8*, 581–583.
- (58) Draine, B. T.; Flatau, P. J. *J. Opt. Soc. Am. A* **1994**, *11*, 1491–1499.
- (59) Johnson, P. B.; Christy, R. W. *Phys. Rev. B* **1972**, *6*, 4370–4379.
- (60) Prescott, S. W.; Mulvaney, P. *J. Appl. Phys.* **2006**, *99*, 123504.
- (61) Jain, P. K.; Lee, K. S.; El-Sayed, I. H.; El-Sayed, M. A. *J. Phys. Chem. B* **2006**, *110*, 7238–7248.
- (62) Coronado, E. A.; Schatz, G. C. *J. Chem. Phys.* **2003**, *119*, 3926–3934.
- (63) Felidj, N.; Aubard, J.; Levi, G. *J. Chem. Phys.* **1999**, *111*, 1195–1208.
- (64) de Abajo, F. J. G. *J. Phys. Chem. C* **2008**, *112*, 17983–17987.
- (65) McMahon, J. M.; Gray, S. K.; Schatz, G. C. *Nano Lett.* **2010**, *10*, 3473–3481.
- (66) Gunnarsson, L.; Rindzevicius, T.; Prikulis, J.; Kasemo, B.; Käll, M.; Zou, S.; Schatz, G. C. *J. Phys. Chem. B* **2005**, *109*, 1079–1087.
- (67) Maier, S. A. *Plasmonics: Fundamentals and Applications*; Springer: New York, 2007.
- (68) Hohenau, A.; Krenn, J. R. *Phys. Rev. B* **2006**, *73*, 155404.
- (69) Jain, P. K.; El-Sayed, M. A. *Chem. Phys. Lett.* **2010**, *487*, 153–164.
- (70) Jain, P. K.; El-Sayed, M. A. *J. Phys. Chem. C* **2008**, *112*, 4954–4960.